Progress In Electromagnetics Research C, Vol. 72, 81–89, 2017

Low-Profile Wideband Circularly Polarized Microstrip Antenna with Conical Radiation Pattern

Dan Yu*, Yang-Tao Wan, and Hao-Bin Zhang

Abstract—A low-profile wideband circularly polarized (CP) microstrip antenna with conical radiation patterns is designed in this paper. Based on the center-fed circular microstrip patch structure, the proposed antenna symmetrically employs 5 shorting vias connecting the patch and the ground plane to provide the θ-polarization and 11 slant sector branches at the edge of circular patch to generate the ϕ-polarization. With the phase difference of 90° between the two orthogonal polarizations, the design radiates right-handed circularly polarized (RHCP) waves. The proposed antenna works at three resonant modes. To realize broad operating bandwidth, the slant sector branches should be carefully adjusted to make the second resonant mode couple the first mode (TM_{01} mode) and third mode (TM_{02} mode) together. The measured results show that the proposed antenna has a low profile of 0.025λ, impedance bandwidth of 35.4% (3.74–5.35 GHz), and axial ratio (AR) bandwidth of 38% (3.7–5.45 GHz). To further verify the characteristics of the proposed antenna, the studies on several important parameters are carried out by HFSS simulation, and a simple design guideline is provided.

1. INTRODUCTION

Omnidirectional circularly polarized (CP) antennas are widely used in modern wireless communication systems for the 360° signal coverage capacity in horizontal plane, stable signal transmission, strong anti-jamming capability, and low polarization mismatch losses. With the wideband demand for high performance and big capacity telecommunication systems, wideband omnidirectional CP antennas have been proposed and investigated over the past few years [1–11]. Working at TM_{21} mode of a circular microstrip antenna, early wideband omnidirectional CP antenna [1] uses a 90° phase shifter and hybrid feeding mechanism to get the broad working bandwidth of 28.2%. Then, omnidirectional CP property is gained by introducing the inclined slots on the sidewalls of a rectangular linear polarized (LP) dielectric resonator antenna (DRA) [2]. Furthermore, the omnidirectional CP antenna in [3] achieves wide operating bandwidth of 25% by embedding a metal parasitic strip on each of the inclined slots of the CP DRA in [2]. Using the parasitic dielectric parallelepiped elements as the wave polarizers which convert omnidirectional LP fields radiated by the probe into CP fields, a CP dielectric bird-nest antenna [4] with conical radiation patterns has a broad operating bandwidth of 41%. Connecting the Alford loop at the edge of the patch, a center-fed circular microstrip patch antenna [5] with mushroom structure can radiate omnidirectional CP waves. By removing the shorting vias of the mushroom structure and increasing the profile of the antenna in [5], a omnidirectional CP DRA [6] has a wider usable bandwidth of 7%. Based on symmetric vortex slots and shorting vias, a center-fed circular microstrip patch antenna can radiate omnidirectional RHCP waves with a usable bandwidth of 51.7% [7].

However, these wideband omnidirectional CP antennas have relatively high profiles, which is not suitable for the space-constrained application [8]. Moreover, the antennas with high profile cannot be used on the objects moving on a bumpy road for large wind resistance and unstable structures. To

Received 11 January 2017, Accepted 24 February 2017, Scheduled 8 March 2017
* Corresponding author: Dan Yu (yudansee@163.com).
The authors are with the China Electronics Technology Group Corporation the 29th Research Institute, 610000, China.

lower the profile of the omnidirectional wideband CP antennas, the designs based on a planar microstrip patch structure have been investigated. Simply consisting of a wideband monopolar patch structure and eight parasitic loop stubs, a wideband CP antenna [8] with conical radiation pattern provides a usable bandwidth of 12.2% and low profile of 0.06λ. Then, with a wide operating bandwidth of 18.4% and low profile of 0.024λ, a center-fed circular microstrip antenna employs shorting vias to achieve wideband impedance matching and connects the curved slots at the edge of circular ground plane to excite a degenerate mode and create CP field [9]. In addition, employing a top-loaded cylindrical monopole for generating omnidirectional vertical polarization and four printed arc-shaped dipoles for generating horizontal polarization, an omnidirectional CP antenna [10] for WLAN access point has a low profile of 0.086λ. With the low profile of 0.076λ, a compact omnidirectional antenna of circular polarization is proposed in [11].

With symmetric structures, all of these omnidirectional wideband CP antennas with low profile use shorting vias or monopoles which function as electric dipoles to produce θ-polarization and employ Alford loop or its transformations which function as magnetic dipoles to provide ϕ-polarization. In [8], the authors indicate that 'there are other ways to introduce a magnetic dipole for developing a CP antenna'. In fact, with a proper selection, the structures which function as magnetic dipoles can also help to enhance the working bandwidth. However, the Alford loop and its transformations are the linear structures which are not good for getting broader bandwidth.

In this paper, we connect slant sector branches, which belong to the gradual faces, symmetrically to the edge of a circular patch of the proposed low-profile wideband CP microstrip antenna for generating ϕ-polarization and broadening the working bandwidth. Employing 5 shorting vias to radiate θ-polarizations, a low-profile wideband conical beam CP antenna based on a center-fed circular patch structure is proposed. The design works at three resonant modes, simultaneously. With careful adjustment of the slant sector branches, the first mode (TM_{01} mode) and the third mode (TM_{02} mode) which are provided by the shorting vias and circular patch [12] can be coupled together by the second resonant mode which is controlled by the slant sector branches. It should be mentioned that the proposed antenna must work with a small ground plane to get a better impedance matching. To demonstrate the idea, the proposed antenna is fabricated and measured. The measured results show that the proposed antenna radiates RHCP waves with the impedance bandwidth of 35.4%, AR bandwidth of 38%, usable bandwidth of 35.4%, and low profile of 0.025λ at the lowest resonant frequency. To express both the broadband and CP principles of the proposed antenna clearly, several vital parameters of the slant sector branches, shorting vias, and ground plane are studied in details. Finally, a simple design guideline and a performance comparison between the related wideband conical beam CP antennas and the proposed antenna are given.

2. ANTENNA DESIGN

Figure 1 shows the configuration of the proposed low-profile wideband conical beam CP antenna. The proposed antenna consists of a circular ground with radius of R_1, a center-fed circular patch with radius of R_2, 11 slant sector branches symmetrically connected at the edge of patch, and 5 shorting vias symmetrically placed on the circle of radius Rv. The radius of each shorting via is r. As shown in Figure 1(a), every slant sector branch is composed of two arcs with their centers at the feeding point. The inner arc has radius of R_2 and length of l_1, while the outer arc has radius of R_3 and length of l_2. The slant sector branches are tilted in the clockwise direction by the angle of α which makes the proposed antenna radiate RHCP waves. It should be mentioned that the proposed antenna radiates LHCP waves when the slant sector branches are tilted in the counterclockwise direction. The proposed microstrip antenna is fabricated on a cylinder substrate with the thickness of 2 mm, radius of R_s, and relative permittivity of 2.65.

Based on the symmetrical structure, the design utilizes shorting vias to provide θ-polarization and employs the slant sector branches to provide ϕ-polarization. When the two orthogonal polarizations are equal in amplitudes but different in phase by 90° [11], the proposed antenna radiates conical beam CP waves. As shown in Figure 2, the currents on the shorting vias are in the direction of $-Z$, and the currents on the slant sector branches are in the direction of $-\phi$. According to [7], the phase of ϕ-polarized wave is always ahead of that of θ-polarized wave by 90°, and the proposed antenna radiates

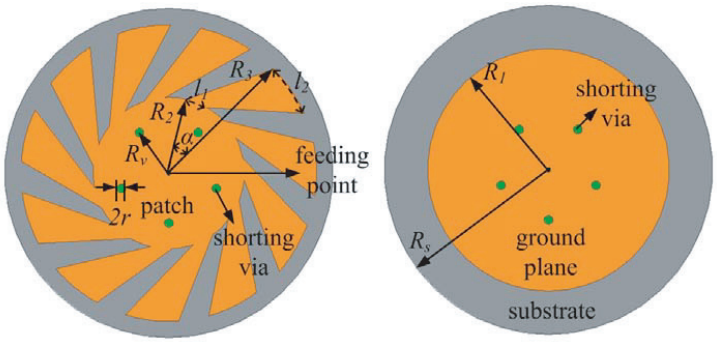

Figure 1. Configuration of the proposed low-profile wideband conical beam CP antenna. (a) Top view. (b) Bottom view.

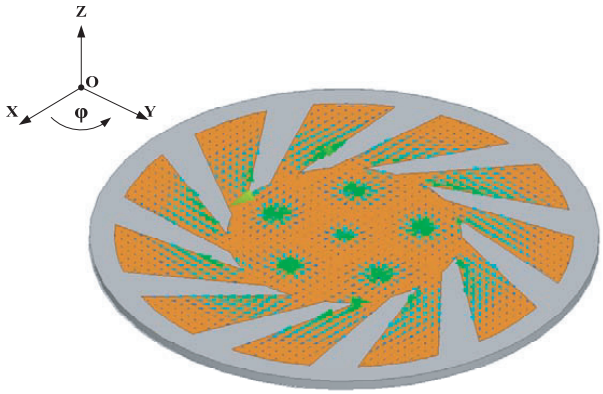

Figure 2. The currents distributions on the patch of the proposed antenna.

RHCP waves in the far field. Because of the introduction of shorting vias, the proposed antenna is excited at TM_{01} and TM_{02} modes of the circular microstrip patch [12]. Moreover, by carefully adjusting the size of the slant sector branches, a middle resonant mode between TM_{01} and TM_{02} modes can couple them together, which brings a wider operating bandwidth of the proposed antenna than that of [8], [9], and [12].

A cylinder cavity model can be used to analyze the circular microstrip antenna with center fed structure. Considering the fringing field at the open edge, the effective radius R_{2eff} of the circular patch can be calculated [12] by

$$R_{2eff} = R_2\sqrt{1+\frac{2h}{\pi R_2\varepsilon_r}\left(\ln\frac{\pi R_2}{2h}+1.7726\right)} \tag{1}$$

where h is the thickness of the proposed antenna.

When the patch is not shorted by the vias, TM_{01} mode resonates at zero. With the introduction of shorting vias, TM_{01} and TM_{02} modes resonate at the closest frequencies and the position of the shorting vias at about

$$R_2 = 0.6276R_{2eff} \tag{2}$$

With the analysis and equations, the proposed wideband patch antenna can be well designed.

3. SIMULATED AND MEASURED RESULTS

The prototype of the proposed low-profile wideband conical beam CP antenna is shown in Figure 3. The parameters are given by $R_1 = 36.8\,\text{mm}$, $R_2 = 23\,\text{mm}$, $R_3 = 45\,\text{mm}$, $Rs = 50\,\text{mm}$, $R_v = 15.2\,\text{mm}$, $r = 1.3\,\text{mm}$, $\alpha = 32^\circ$, $l_1 = 6.62\,\text{mm}$, and $l_2 = 16.33\,\text{mm}$.

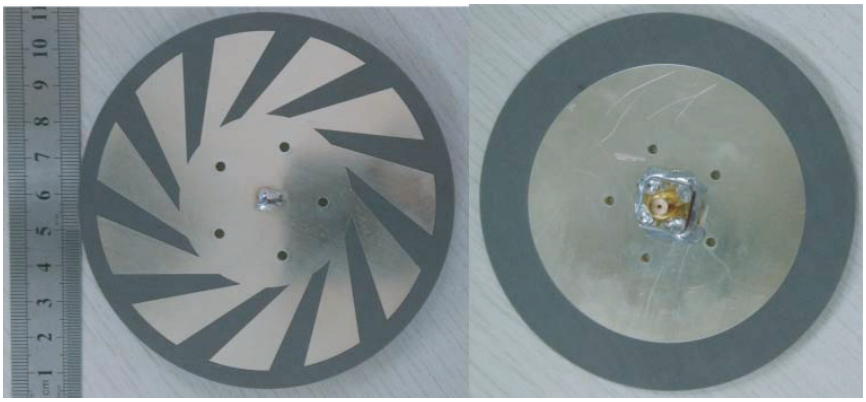

(a) (b)

Figure 3. The prototype of the low-profile wideband conical beam CP antenna. (a) The photography showing the patch view of the proposed antenna. (b) The photography showing the ground view of the proposed antenna.

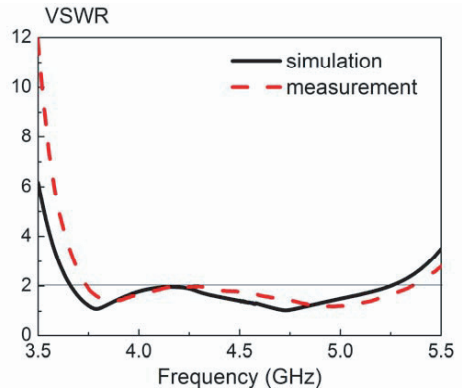

Figure 4. Simulated and measured voltage standing wave ratio (VSWR) of the proposed antenna.

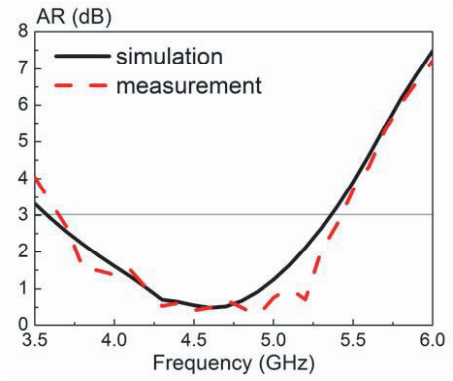

Figure 5. Simulated and measured ARs of the prototype at $\theta = 30°$ and $\phi = 0°$.

As shown in Figure 4, the measured impedance bandwidth (VSWR < 2) of the proposed antenna is 35.4% (3.74–5.35 GHz) which agrees well with the simulated result of 35.4% (3.66–5.25 GHz). It should be noticed that the measured resonant frequency is little higher than the simulated result for the fabrication tolerance. With reference to the figure, the proposed antenna operates at three modes, and the middle mode (4.9 GHz) which is controlled by the slant sector branches is closer to the third mode (5.25 GHz) than to the first mode (3.85 GHz). Furthermore, the first and third modes correspond to TM_{01} and TM_{02} modes, respectively, which are analyzed in detail in [12].

The simulated and measured ARs of the proposed prototype at $\theta = 30°$ and $\phi = 0°$ are shown in Figure 5. With reference to the figure, the measured 3-dB AR bandwidth of the proposed antenna is 38% (3.7–5.45 GHz) which agrees well with the simulated result of 39.1% (3.6–5.35 GHz). Compared with Figure 4, the measured 3-dB AR bandwidth completely covers the measured impedance bandwidth, and the usable bandwidth of 35.4% (3.75–5.35 GHz) is achieved. Such a usable bandwidth is sufficient for many wireless systems. ARs are also simulated and measured at other values of ϕ with $\theta = 30°$, and similar results are obtained.

Figure 6 shows the simulated and measured radiation patterns of the proposed antenna in the elevation ($\phi = 0°$) and azimuth ($\theta = 30°$) planes at three resonant modes. It is clearly seen that the elevation patterns in the left have two nulls in the boresight directions ($\theta = 0°$ and $\theta = 180°$) while the azimuth patterns in the right are conical with the maximum radiation angle of $\theta = 30°$ at all the

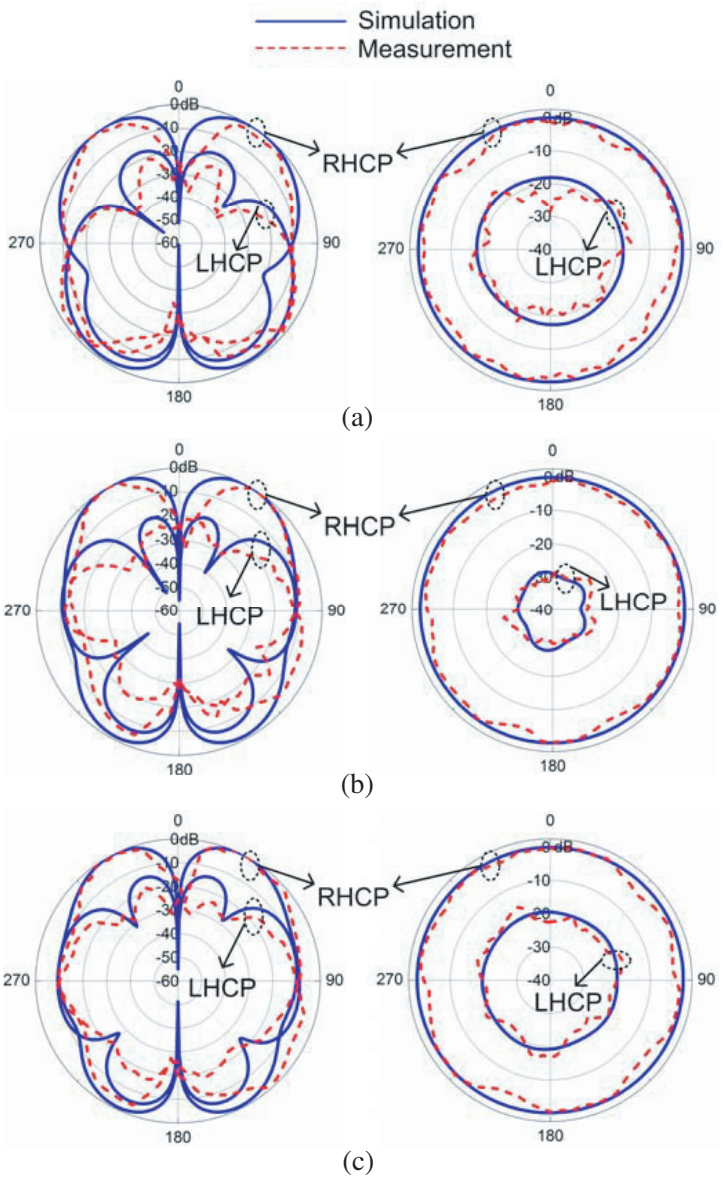

Figure 6. Simulated and measured radiation patterns in the elevation (left) and azimuth (right) planes at (a) 3.85 GHz, (b) 4.9 GHz, and (c) 5.25 GHz.

three modes. In the azimuth plane ($\theta = 30°$), the proposed antenna radiates RHCP waves stronger than LHCP waves by 15 dB at least. The radiation patterns in the elevation plane at other values of ϕ are simulated and measured at all the three modes, and similar results are obtained showing good omnidirectional property of the proposed antenna. This is because of the symmetric structure of the proposed antenna. The measured peak gains of the proposed antenna at three resonant frequencies are 3.2 dBic, 4.2 dBic, and 3.6 dBic, respectively, which are smaller than the gains of the wideband omnidirectional CP antennas in [1] and [4] for the smaller ground plane.

4. PARAMETRIC STUDY

To verify the properties of the design, several vital parameters of the proposed antenna are analyzed in details. We use HFSS 15 software for the simulation. It should be mentioned that only one parameter changes each time with the other parameters same as the fabricated prototype shown in Figure 3.

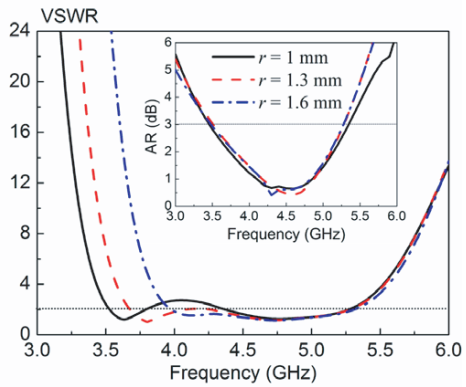

Figure 7. Simulated VSWR of the proposed antenna with different r. The inset shows the corresponding ARs at $\theta = 30°$ and $\phi = 0°$.

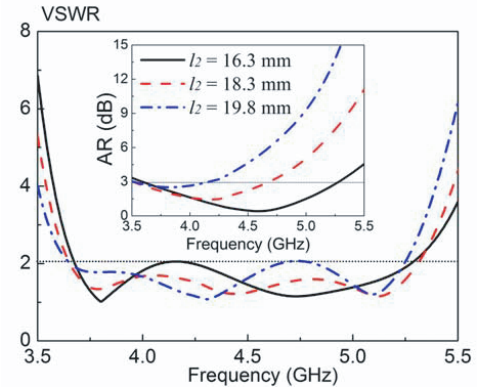

Figure 8. Simulated VSWR of the proposed antenna with different l_2. The inset shows the corresponding ARs at $\theta = 30°$ and $\phi = 0°$.

Firstly, to realize broad operating bandwidth, the first mode (TM_{01} mode) should be designed far apart from the third mode (TM_{02} mode). Therefore, the effects of radius r of the shorting vias on TM_{01} and TM_{02} modes are studied. Figure 7 shows the simulated VSWR and corresponding ARs of the proposed antenna with different radii of the shorting vias. With reference to the figure, the resonant frequency of the first mode which corresponds to TM_{01} mode decreases with the decrease of r for the increase of the currents path [12], while the resonant frequencies of the second and third modes (TM_{02} mode) keep unchanged. As shown in the inset, the corresponding ARs keep almost unchanged, which indicates that the distance between TM_{01} and TM_{02} modes can be adjusted freely without worrying about the ARs.

After determining the resonant frequencies of TM_{01} and TM_{02} modes, the middle mode which is controlled by the slant sector branches should be adjusted to couple the two modes together for getting wider operating bandwidth. Therefore, the parameters (l_2 and α) of the slant sector branches are studied.

Figure 8 shows the simulated VSWR and corresponding ARs of the proposed antenna with different l_2. With reference to the figure, the resonant frequency of the middle mode decreases with the increase of l_2, while the resonant frequencies of the first and third modes remain unchanged. This is because the middle mode is mainly controlled by the slant sector branches whose areas increase with the increase of l_2. As shown in the inset, the corresponding ARs at $\theta = 30°$ and $\phi = 0°$ increase with the increase of l_2 due to the changing of the ϕ-polarization which is provided by the slant sector branches. Therefore, to get broad AR bandwidth, the middle mode of the fabricated prototype is closer to the third mode than to the first one.

Different from the wideband CP antenna in [9], the slant sector branches which are responsible for the CP field are connected to the radiating patch instead of the ground plane. This means that the slant sector branches will have significant effect on the input impedance of the proposed antenna. Figure 9 shows the simulated VSWR and corresponding ARs of the design with different tilted angles α of the slant sector branches. With reference to the figure, VSWR increases rapidly with the decrease of α. As shown in the inset, the corresponding ARs of the proposed antenna increase with the decrease of α for the reason that the ϕ-polarization which is radiated by the slant sector branches weakens with the decrease of α.

With the two parametric studies above, the slant sector branches have significant effect on both the impedance and AR properties. Therefore, the sector branches should be carefully designed for both wide impedance bandwidth and wide AR bandwidth.

To achieve both low profile and wide operating bandwidth, the proposed antenna should employ a smaller ground plane to lower its quality factor (Q) [7]. Therefore, the radius of the ground plane has also been analyzed. Figure 10 shows the simulated VSWR and corresponding ARs of the proposed antenna with different radii of the ground plane. With reference to the figure, the resonant depths of all the three modes become shallow with the increase of R_1 due to the higher Q value. As shown in

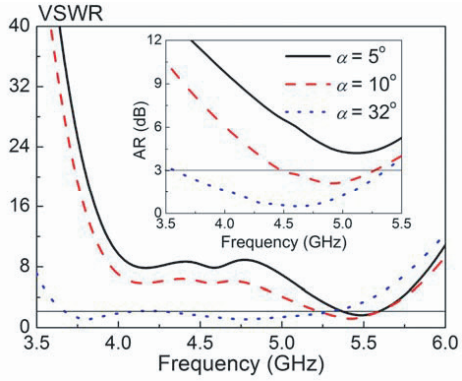

Figure 9. Simulated VSWR of the proposed antenna with different α. The insect shows the corresponding ARs at $\theta = 30°$ and $\phi = 0°$.

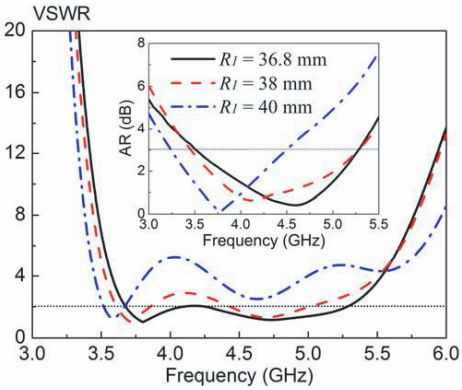

Figure 10. Simulated VSWR of the proposed antenna with different R_1. The inset shows the corresponding ARs at $\theta = 30°$ and $\phi = 0°$.

the inset, the corresponding AR bandwidth shifts downwards with the increase of R_1. Therefore, the optimum radius of the ground plane is given by 36.8 mm.

A simple design guideline of the proposed antenna is given as follows: First, with the certain resonant frequencies of the first mode (TM_{01} mode) and third mode (TM_{02} mode), the parameters of the circular patch and shorting vias can be designed by using the principle presented in [12]. It should be mentioned that the two resonant frequencies should be designed far apart to get the wide impedance bandwidth. Then, according to the parametric studies shown in Figure 8 and Figure 9, the slant sector branches should be properly designed to make the second mode couple TM_{01} and TM_{02} modes together and get a wide AR bandwidth. Furthermore, the radius of the ground plane should be decreased to get

Table 1. Comparison of various wideband conical beam CP antennas.

	Impedance bandwidth	AR bandwidth	Usable bandwidth	Max-gain dBic
[1]	28.2%	32.9%	28.2%	5.5
[4]	41%	54.9%	41%	5
[8]	28%	14.4%	12.2%	4.9
[9]	19.8%	19.3%	18.4%	4.68
[13]	–	33.6%	33.6%	8.5
[14]	37%	22%	22%	5.8
Proposed antenna	35.4%	38%	35.4%	4.2

	Cross section	Profile	ε_s	Feeding method
[1]	$2.70\lambda \times 2.70\lambda$	0.10λ	1.0	Hybrid feeding network
[4]	$1.15\lambda \times 1.15\lambda$	0.55λ	15	Coaxial feed
[8]	$1.16\lambda \times 1.16\lambda$	0.06λ	2.94	Coaxial feed
[9]	$1.36\lambda \times 1.36\lambda$	0.024λ	2.2	Coaxial feed
[13]	$0.52\lambda \times 0.52\lambda$	0.228λ	2.2	Microstrip line
[14]	$0.87\lambda \times 0.87\lambda$	0.212λ	10.2	Microstrip line
Proposed antenna	$1.25\lambda \times 1.25\lambda$	0.025λ	2.65	Coaxial feed

a better impedance matching of all the three resonant modes. Finally, a particular optimization may be carried out by fine-tuning each parameter.

To further show the properties of the proposed antenna, a comparison of related wideband conical beam CP antenna with the proposed antenna is made in Table 1. With reference to the table, all the impedance, AR, and usable bandwidths of the proposed antenna are wider than those of the wideband CP antenna in [1, 8, 9, 13, 14] but narrower than those of the antenna in [4]. However, the profile of the proposed antenna is 20 times lower than that in [4]. With the small ground plane, the maximum gain of the proposed antenna is smaller than those in above references. Compared with the low-profile wideband conical beam CP antennas in [8] and [9], the proposed antenna has much wider impedance, AR, and usable bandwidths. Additionally, the profile of the proposed antenna is much lower than that in [8] but little higher than that in [9]. The antennas in [13] and [14] have greater peak gains than ours, for the directional radiation pattern, and their structures are not stable for the multi-layers and the separate trapezoidal patch. In summary, the proposed low-profile wideband CP antenna has obvious advantages among the related wideband conical beam CP antennas.

5. CONCLUSION

A low-profile wideband CP antenna with conical radiation pattern is investigated and fabricated in this paper. Based on the symmetric structure, the proposed antenna employs shorting vias and slant sector branches to obtain the broadband CP radiation field. The proposed antenna operates at three modes which include TM_{01} mode, TM_{02} mode, and a middle mode between them. To achieve a broad working bandwidth, TM_{01} and TM_{02} modes of the proposed antenna should be designed far apart from each other. Then, the middle mode which is controlled by the slant sector branches is adjusted properly to couple the first and the third modes together. The measured results show that the proposed antenna radiates RHCP waves with the impedance bandwidth of 35.4%, AR bandwidth of 38%, usable bandwidth of 35.4%, and low profile of 0.025λ. Important parameters are analyzed to verify the design, and a simple design guideline is given. Finally, a comparison of the properties between the proposed antenna and relative wideband CP antenna is carried out to show its advantages.

REFERENCES

1. Lau, K. L. and K. M. Luk, "A wideband circularly polarized conical-beam patch antenna," *IEEE Trans. Antennas Propag.*, Vol. 54, No. 5, 1591–1594, May 2006.
2. Pan, Y. M., K. W. Leung, and K. Lu, "Omnidirectional linearly and circularly polarized rectangular dielectric resonant antennas," *IEEE Trans. Antennas Propag.*, Vol. 60, No. 2, 751–759, Feb. 2012.
3. Pan, Y. M. and K. W. Leung, "Wideband omnidirectional circularly polarized dielectric resonator antenna with parasitic strips," *IEEE Trans. Antennas Propag.*, Vol. 60, No. 6, Jun. 2012.
4. Pan, Y. M. and K. W. Leung, "Wideband circularly polarized dielectric bird-nest antenna with conical radiation pattern," *IEEE Trans. Antennas Propag.*, Vol. 61, No. 2, 563–570, 2013.
5. Park, B. C. and J. H. Lee, "Omnidirectional circularly polarized antenna utilizing zeroth-order resonance of epsilon negative transmission line," *IEEE Trans. Antennas Propag.*, Vol. 59, No. 7, 2717–2721, 2011.
6. Li, W. W. and K. W. Leung, "Omnidirectional circularly polarized dielectric resonator antenna with top-loaded Alford loop for pattern diversity design," *IEEE Trans. Antennas Propag.*, Vol. 61, No. 8, 4246–4256, Aug. 2013.
7. Yu, D., S. X. Gong, Y. T. Wan, Y. L. Yao, Y. X. Xu, and F. W. Wang, "Wideband omnidirectional circularly polarized patch antenna based on vertex slots and shorting vias," *IEEE Trans. Antennas Propag.*, Vol. 62, No. 8, 3970–3977, Aug. 2014.
8. Lin, W. and H. Wong, "Circularly-polarized conical-beam antenna with wide bandwidth and low profile," *IEEE Trans. Antennas Propag.*, Sep. 2014.
9. Pan, Y. M., S. Y. Zheng, and B. J. Hu, "Wideband and low-profile omnidirectional circularly polarized patch antenna," *IEEE Trans. Antennas Propag.*, Vol. 62, No. 8, 4347–4351, Aug. 2014.

10. Hsiao, F. R. and K. L. Wong, "Low-profile omnidirectional circularly polarized antenna for WLAN access point," *Microw. Opt. Technol. Lett.*, Vol. 46, No. 3, 227–231, 2005.
11. Yu, Y. F., Z. X. Shen, and S. L. He, "Compact omnidirectional antenna of circular polarization," *IEEE Trans. Antennas Wireless Propagat. Lett.*, Vol. 11, 1466–1469, 2012.
12. Liu, J. H., Q. Xue, H. Wong, H. W. Lai, and Y. L. Long, "Design and analysis of a low-profile and broadband microstrip monopolar patch antenna," *IEEE Trans. Antennas Propag.*, Vol. 61, No. 1, 11–18, Jan. 2013.
13. Oraizi, H. and R. Pazoki, "Wideband circularly polarized aperture-fed rotated stacked patch antenna," *IEEE Trans. Antennas Propag.*, Vol. 61, No. 3, 1048–1054, Mar. 2013.
14. Fakhte, S., H. Oraizi, R. Karimian, and R. Fakhte, "A new wideband circularly polarized stair-shaped dielectric resonator antenna," *IEEE Trans. Antennas Propag.*, Vol. 63, No. 4, 1828–1831, Apr. 2015.